

PAPER • OPEN ACCESS

Numerical analysis of erosion due to nanoparticles in a pipe elbow

To cite this article: Anna Kosinska and Boris V. Balakin 2018 *J. Phys.: Conf. Ser.* **1133** 012045

View the [article online](#) for updates and enhancements.



IOP | ebooks™

Bringing you innovative digital publishing with leading voices to create your essential collection of books in STEM research.

Start exploring the [collection](#) - download the first chapter of every title for free.

Numerical analysis of erosion due to nanoparticles in a pipe elbow

Anna Kosinska¹, Boris V. Balakin^{1,2}

¹ Western Norway University of Applied Sciences, Inndalsveien 28, 5063 Bergen, Norway

² NRNU Moscow Engineering Physics Institute, Kashirskoe shosse, 31, 115409 Moscow, Russia

E-mail: adk@hv1.no

Abstract. Flows of fluids laden with small particles in pipes are common in industry. An interesting and still unexplored issue is erosion of walls due to impact of particles. The main focus of our research was on nanoparticles. This type of particles have recently been tested as e.g. potential components of coolants. In this paper, attention was paid to erosion due to particles through pipe elbows. It was discovered that while smaller particle should result in essentially lower erosion rate, this does not always occur. Smaller particles tend namely to move faster towards the wall due to vortices, which may enhance the erosion.

1. Introduction

Transportation of particles in fluids through pipes may lead to significant wear of the wall material. The degree of erosion depends on factors such as particle size, material, velocity and pipe geometry. Recently, researchers have begun to focus on the most common pipe geometry, that is, elbows, see e.g. [1–20]. In the following, we show a short description of some selected works.

Peng and Cao [9] combined five different erosion models and two particle-wall rebound models to predict the erosion rate and the maximum erosion location. According to their research, two of the models (so-called Erosion/Corrosion Research Center model and the Grant and Tabakoff model) produced results that compared well with experiments. Similarly, Pereira et al. [1] examined that model proposed by Oka et al. gives the best results for erosion prediction.

Liu et al. [14] measured experimentally erosion-corrosion rate at different positions of a horizontal steel piping elbow. Duarte et al. [13] paid attention to the details of the mathematical model and considered issues such as particle-particle interactions. Obviously, this phenomenon plays a role when the particle loadings are high. Also, Sorndal et al. [2] took into account the roughness of the wall. They discovered that assumption of smooth walls in the model may lead to non-physical results. Xu et al. [11] considered parameters such as friction coefficient and coefficient of restitution for particle-particle interactions. They showed that changing of these parameters does not influence the results significantly. Zhou et al. [20] looked into the effects of particle shape and swirling intensity.

Finally, an interesting possibility was examined by Duarte et al. [8]: the elbow was equipped by an additional vortex chamber so that particle-wall collisions were less severe. As a results the erosion rate was lower.



Even though the issue of particle erosion on multiphase flows through elbows have been intensively researched, less attention was paid to flows of nanofluids, i.e., fluids with immersed nanoparticles. These types of fluids have gained much interest in the past years as they show enhanced heat transfer properties when compared to “pure” fluids. Therefore they can be used e.g. in cooling systems in combustion engines or as coolants in nuclear reactors.

It may be, however, questionable whether use of nanoparticles does not result in wear of pipe material. Therefore, in this paper, we investigate numerically erosion process of nanofluids flow through a pipe with an elbow. Our tool is the computational fluid dynamics (CFD) and we used the commercial software Star-CCM+.

2. Problem description

The geometry of a typical elbow used in industry is shown in Figure 1 and such a geometry was also used in our research. The geometry and the dimensions were inspired by Duarte et al. [8].

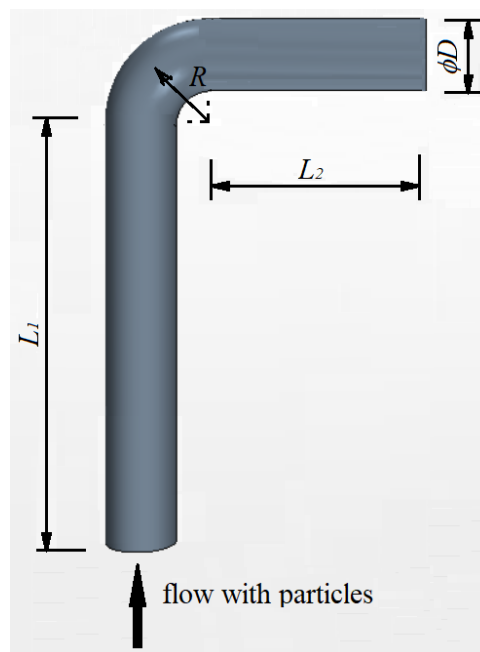


Figure 1. The scheme of the computational domain

The flow laden with particles is injected to the lowest pipe, as shown in Figure 1. The pipe diameter D , and the curvature R are 0.0508 m (= 2 in.), the lengths L_1 and L_2 are 0.3048 m and 0.1524 m, respectively. It must be noted that especially L_1 has to be large enough to ensure a well-developed flow not influenced by the boundary conditions. The velocity at the inlet was for both cases equal to 1.0 m/s.

The fluid had the properties of air with density $\rho = 1.225 \text{ kg/m}^3$ and dynamic viscosity $\mu = 1.79 \cdot 10^{-5} \text{ Pa}\cdot\text{s}$. The particle material density was 2600 kg/m^3 .

Different particle diameters were tested in this research, where the smallest particles had the diameter 10^{-8} m (nano-range), and the largest particles had a diameter 10^{-4} m . The particles were spherical.

The particles were injected with a volume flow rate $6.45 \cdot 10^{-5} \text{ m}^3/\text{s}$. For this value the volume fraction of the particulate was low so that particle-particle collisions could be ignored. The process was unsteady, that is, there were no particles in the system at the beginning as well

as the initial velocity was zero. The total simulation time was 1.4 s. The flow became steady before this time.

3. Mathematical model

It is assumed that the flow of the fluid is governed by the standard equations of continuity and momentum, i.e.:

$$\frac{\partial \phi_c \rho_c}{\partial t} + \nabla \cdot (\phi_c \rho_c \mathbf{u}) = 0 \quad (1)$$

$$\frac{\partial \phi_c \rho_c \mathbf{u}}{\partial t} + \nabla \cdot (\phi_c \rho_c \mathbf{u} \mathbf{u}) = -\phi_c \nabla p + \nabla \cdot (\phi_c (\tau + \tau^t)) - f_\Sigma, \quad (2)$$

where ρ_c is density, ϕ_c is the volume fraction, \mathbf{u} is velocity, p is pressure, τ and τ^t is the molecular and shear stress tensor, respectively.

In addition, f_Σ accounts for the interphase momentum transfer, which is due the interphase forces (see below). In other words, we choose the two-coupling between the phases. Some authors, e.g. [8, 11, 13], have compared the influence of the one-way coupling and two-way coupling on the erosion rate when investigating flows with particles through pipes. Usually, the difference was not significant. For modelling of turbulence, we chose the standard k - ϵ model.

For modelling of the particles we used the Lagrangian approach, that is, the particles are tracked individually in the computational domain. Thus, the behaviour of each particles can be described using:

$$m_i \frac{d\mathbf{v}_i}{dt} = \Sigma \mathbf{F}, \quad (3)$$

where: i denotes i -th particle, m is the particle mass, \mathbf{v} is particle velocity and $\Sigma \mathbf{F}$ denotes forces acting on the particles. The latter is due to the drag force (modelled using the standard Schiller-Naumann model) and the Saffman lift force [21].

As previously mentioned, particle-particle collisions were not considered in the model since the flow was dilute. Nevertheless, the particle-wall collisions were modelled using a standard hard-sphere model using the coefficient of restitutions along the normal and tangential to the plane of impact. Both parameters were selected to be 0.993, that is, the collision was almost elastic.

The particle erosion with the wall of the pipe was modelled using the OKA model, see [22] and [23]. In this model we calculate the erosion rate that is the mass of wall eroded per unit area and per unit time, which occurs after a particle-wall collision:

$$E_f = \frac{1}{A_f} \sum \dot{m} e_r, \quad (4)$$

where A_f is the area of the face subjected to collisions, \dot{m} is the mass flow rate of particles colliding with the face and e_r is so-called erosion ratio. The erosion ratio is calculated according to [22] as:

$$e_r = (\sin \alpha)^{n_1} (1 + Hv(1 - \sin \alpha))^{n_2} K \left(\frac{v_{rel}}{v_{ref}} \right)^{k_2} \left(\frac{D}{D_{ref}} \right)^{k_3}, \quad (5)$$

where n_1 , n_2 , K , k_2 and k_3 are empirical constants, Hv is material hardness measured in GPa, v_{rel} is the relative velocity of the particle with respect to the wall (along the normal to the impact plane), v_{ref} and D_{ref} are some reference values of velocity and diameter and α is the impact angle (measured from the normal to the impact plane).

In this research the following constants were selected for simulations: $n_1 = 0.74$, $n_2 = 1.823$, $Hv = 1.34$ GPa, $K = 2.14 \cdot 10^{-4}$, $v_{ref} = 104$ m/s, $k_2 = 2.33$, $D_{ref} = 3.26 \cdot 10^{-4}$ m and $k_3 = 0.19$. The values were inspired by the paper by Oka [22] and did not vary in the present research.

4. Results and discussion

At first we focus on the overall erosion rate (dimensions: eroded mass per time) at the end of the simulations, that is, when the flow becomes steady. Figure 2 shows the relation between the overall erosion rate and particle diameter.

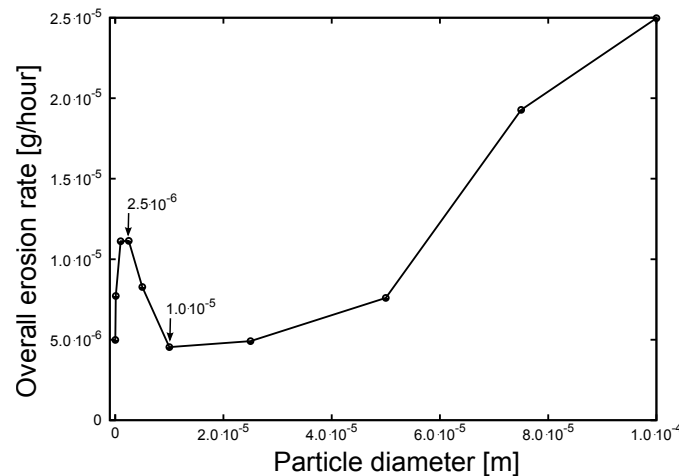


Figure 2. Overall erosion rate vs. particle diameter

For large particle size we observe an obvious trend, i.e. larger particles lead to higher erosion. Nevertheless, this changes for lower diameters where the overall erosion rate suddenly increased to a certain value (corresponding to particle diameter $\approx 2.5 \cdot 10^{-6}$ m) and then decreased again for the smallest particles.

The first explanation of this counter-intuitive phenomenon is the fact that the total number of particles increased when the particle size decreased. It must be noted that the volume fraction was the same in all simulations while the diameter varied. The higher number of particles resulted in more frequent collisions so that the overall erosion rate also increased. On the other hand, this reasoning does not explain the fact that for very low particle diameters, the erosion rate became decreases again. Therefore, in the following, we investigate this issue more thoroughly.

Figure 3 shows erosion rate distribution for three particle diameters: $1.0 \cdot 10^{-4}$ m, $1.0 \cdot 10^{-5}$ m and $2.5 \cdot 10^{-6}$ m. These three diameters correspond respectively to the three cases: (i) the highest overall erosion rate detected in our simulations; (ii) the lowest overall erosion rate; (iii) the local increase in the overall erosion rate.

Case (i) refers to the highest overall erosion rate due to the largest particle size. A distribution of erosion rate is shown in Figure 3a. The first observation is that the highest erosion occurs on the outer side of the elbow (i.e. the extrados), which is due to the fact that the largest particles have also the largest inertia. This can also be confirmed by a simple analysis: diameter 10^{-4} m corresponds to the momentum response time (see e.g. [21]) equal to 0.08 s (using the particle and fluid properties shown above). Assuming the characteristic flow time to be 0.0254 s (considering the average flow velocity and pipe diameter), this results in the Stokes number being 3.15, i.e. larger than 1.0.

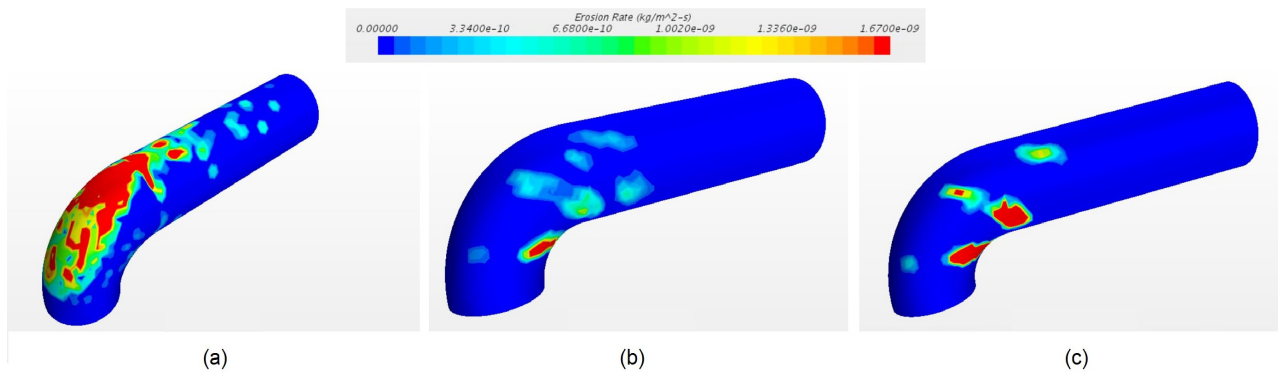


Figure 3. Distribution of erosion rate in the elbow and in the downstream section of the pipe for three values of particle diameter: (a) $1.0 \cdot 10^{-4}$ m, (b) $1.0 \cdot 10^{-5}$ m, (c) $2.5 \cdot 10^{-6}$ m. The results correspond to the time 1.4 s, i.e. after the process achieved a steady state.

Case (ii) is shown in Figure 3b, where the erosion rate is also much lower. This supports what can be detected in Figure 2. This time, however, we observe that the highest erosion rate occurs close to the inner side of the elbow (i.e. intrados). Similarly, Case (iii) is shown in Figure 3c, where the erosion rate is clearly higher than for Case (ii).

A similar theoretical analysis as was done for Case (i) can also be performed for Case (iii). Here the Stokes number becomes $2 \cdot 10^{-3}$, i.e. much lower than 1.0. This indicates that the particles will track the flow.

In order to illustrate this issue, Figure 4 shows fluid velocity distribution in a plane section in the elbow. The plane section is oriented perpendicularly to the pipe centreline. A system of vortices occurs (Dean vortices) that distributes the flow towards the pipe walls. It must be noted that particles are subjected to the flow direction change, especially for the case when the Stokes number was small, that is, for the smallest particles. This indicates that the particles lead to additional erosion close to the intrados. This phenomenon does not occur for the largest particles, associated with the highest Stokes number that pass through the system of vortices unaffected.

5. Conclusions

This paper is devoted to the topic of fluid flows with particles in an elbow. We paid attention to the issue of pipe wall erosion due to the particles. Of special interest are the particles of low diameter, especially in the nano-range.

For the particles of the lowest diameter two opposite phenomena occur. The rate of erosion is essentially low due to the limited size of the particles. This would indicate that the flows with nanoparticles are relatively safe and will result in only limited damage of the pipe. Indeed, our research confirms that the lowest studied particle diameter (10^{-8} m) led to a low erosion rate.

On the other hand, the smallest particles easier migrate towards the wall due to a system of vortices in the fluid. This results in more frequent particle-wall collisions, that is, increased erosion rate.

In this research, we discovered that for a certain range of size of the small particles, the erosion rate increases so that these particles will damage the wall faster than larger particles that migrate less to the pipe wall.

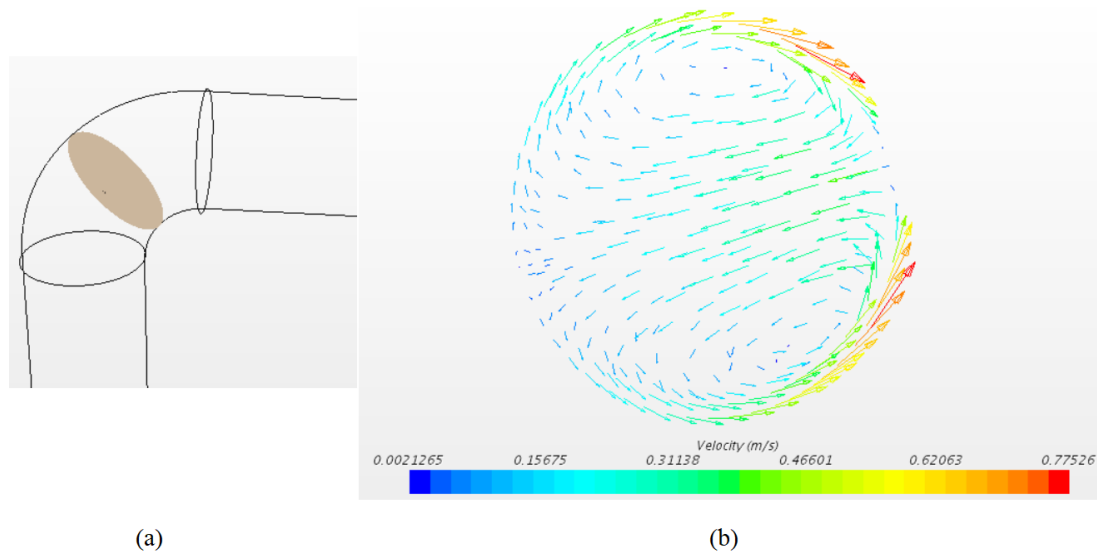


Figure 4. Distribution of fluid velocity field (b) in a plane section oriented perpendicularly to the pipe centreline. The plane is located in the elbow as shown in (a). The results correspond to the time 1.4 s, i.e. after the process achieved a steady state.

6. Acknowledgments

This study was supported by Russian Science Foundation (project 17-79-10481).

References

- [1] Pereira G, de Souza F and de Moro Martins D 2014 *Powder Technol.* **261** 105–117
- [2] Solnordal C, Wong C and Boulanger J 2015 *Wear* **336-337** 43–57
- [3] Lin N, Lan H, Xu Y, Dong S and Barber G 2015 *J. Nat. Gas Sci. Eng.* **26** 581–586
- [4] Mansouri A, Arabnejad H, Shirazi S and McLaury B 2015 *Wear* **332-333** 1090–1097
- [5] Parsi M, MAgrawal, Srinivasan V, Vieira R, Torres C, McLaury B and Shirazi S 2015 *J. Nat. Gas Sci. Eng.* **27** 706–718
- [6] Parsi M, Kara M, Agrawal M, Kesana N, Jatale A, Sharma P and Shirazi S 2017 *Wear* **376-377** 1176–1184
- [7] Shamsirband S, Malvandi A, Karimipour A, Goodarzi M, Afrand M, Petkovic D, Dahari M and Mahmoodian N 2015 *Powder Technol.* **284** 336–343
- [8] Duarte C, de Souza F and dos Santos V 2016 *Powder Technol.* **288** 6–25
- [9] Peng W and Cao X 2016 *Powder Technol.* **294** 266–279
- [10] Peng W and Cao X 2016 *J. Nat. Gas Sci. Eng.* **30** 455–470
- [11] Xu L, Zhang Q, Zheng J and Zhao Y 2016 *Powder Technol.* **302** 236–246
- [12] Zhang J, JKang, Fan J and Gao J 2016 *J. Nat. Gas Sci. Eng.* **32** 334–346
- [13] Duarte C, de Souza F, Salvo R and dos Santos V 2017 *Int. J. Multiphas. Flow* **89** 1–22
- [14] Liu J, Bakedashi W, Li Z, Xu Y, Ji W, Zhang C, Cui G and Zhang R 2017 *Wear* **376-377** 516–525
- [15] Pouraria H, Seo J and Paik J 2017 *Ships Offshore Struc.* **12** 233–243
- [16] Parsi M, Al-Sarkhi A, Kara M, Sharma P, McLaury B and Shirazi S 2017 *Wear* **390-391** 80–83
- [17] Song X, Luo P, Luo S, Huang S and Wang Z 2017 *Adv. Mech. Eng.* **9(10)** 1–18
- [18] Vieira R, Parsi M, Zahedi P, McLaury B and Shirazi S 2017 *Powder Technol.* **320** 625–636
- [19] Wang K, Li X, Wang Y and He R 2017 *Powder Technol.* **314** 490–499
- [20] Zhou J, Liu Y, Liu S, Du C and Li J 2017 *Wear* **380-381** 66–77
- [21] Crowe C, Sommerfeld M and Tsuji Y 1998 *Multiphase Flow with Droplets and Particles* (CRC Press)
- [22] Oka Y, Okamura K and Yoshida T 2005 *Wear* **259** 95–101
- [23] Oka Y and Yoshida T 2005 *Wear* **259** 102–109